The Cryosphere Discuss., 6, 2751–2788, 2012
www.the-cryosphere-discuss.net/6/2751/2012/
doi:10.5194/tcd-6-2751-2012


The Cryosphere Discussions



# A computationally efficient model for the Greenland ice sheet

**J. Haqq-Misra[1,*], P. Applegate[2,3], B. Tuttle[4], R. Nicholas[2], and K. Keller[2]**

[1]Rock Ethics Institute, Pennsylvania State University, University Park, PA, USA
[2]Department of Geosciences, Pennsylvania State University, University Park, PA, USA
[3]Department of Physical Geography and Quaternary Geology (INK), Stockholm University, Stockholm, Sweden
[4]Graduate Program in Acoustics, Pennsylvania State University, University Park, PA, USA
[*]now at: Blue Marble Space Institute of Science, Seattle, WA, USA

Received: 8 June 2012 – Accepted: 22 June 2012 – Published: 23 July 2012

Correspondence to: J. Haqq-Misra (jacob@bmsis.org)

Published by Copernicus Publications on behalf of the European Geosciences Union.

## Abstract

We present a one-dimensional model of the Greenland Ice Sheet (GIS) for use in analysis of future sea level rise. Simulations using complex three-dimensional models suggest that the GIS may respond in a nonlinear manner to anthropogenic climate forcing and cause potentially nontrivial sea level rise. These GIS projections are, however, deeply uncertain. Analyzing these uncertainties is complicated by the substantial computational demand of the current generation of complex three-dimensional GIS models. As a result, it is typically computationally infeasible to perform the large number of model evaluations required to carefully explore a multi-dimensional parameter space, to fuse models with observational constraints, or to assess risk-management strategies in Integrated Assessment Models (IAMs) of climate change.

Here we introduce GLISTEN (GreenLand Ice Sheet ENhanced), a computationally efficient, mechanistically based, one-dimensional flow-line model of GIS mass balance capable of reproducing key instrumental and paleo-observations as well as emulating more complex models. GLISTEN is based on a simple model developed by Pattyn (2006). We have updated and extended this original model by improving its computational functionality and representation of physical processes such as precipitation, ablation, and basal sliding. The computational efficiency of GLISTEN enables a systematic and extensive analysis of the GIS behavior across a wide range of relevant parameters and can be used to represent a potential GIS threshold response in IAMs. We demonstrate the utility of GLISTEN by performing a pre-calibration and analysis. We find that the added representation of processes in GLISTEN, along with pre-calibration of the model, considerably improves the hindcast skill of paleo-observations.

## 1 Introduction

The Greenland Ice Sheet (GIS) is a major feature of the Arctic and exerts a potentially important control on future sea level change. The ice sheet covers an area of

$1.7 \times 10^6$ km$^2$ (Bamber et al., 2001), and has a maximum elevation of ∼3.3 km above sea level (Ekholm, 1996). Its reflective surface and height exert an important control over middle to high northern latitude climates (Toniazzo et al., 2004; Lunt et al., 2004). If the GIS were to melt completely, global sea level would rise by an average of approximately seven meters (Bamber et al., 2001). Although Antarctica holds more ice (∼60 m sea level equivalent; Lythe et al., 2001), Greenland is often considered a more immediate concern because large parts of its surface are already melting (Mote et al., 2007). In contrast, surface melting in Antarctica is largely restricted to the Antarctic Peninsula (Torinesi et al., 2003). Satellite measurements suggest that the GIS mass balance is already negative, and this negative trend may be accelerating (Velicogna, 2009; Alley et al., 2010, and references therein).

Ice sheet model development has been particularly intensive since the Intergovernmental Panel on Climate Change's Fourth Assessment (Meehl et al., 2007), and many modeling experiments have analyzed the past and possible future behavior of the ice sheet (e.g. Greve, 1997, 2000; Huybrechts and de Wolde, 1999; Tarasov and Peltier, 2003; Lhomme et al., 2005; Stone et al., 2010; Greve et al., 2011; Robinson et al., 2011). Many GIS models are "shallow ice" approximation models, with representations of processes that are considered most significant in the real ice sheet. These models neglect important stress components within the ice body (Kirchner et al., 2011). Development and testing of models that resolve these additional stress terms is an area of active research (e.g. Larour et al., 2012).

Although much effort today is given to the development of complex models, simplified but mechanistically based models can play an important role. In particular, integrated assessment models (IAMs) that describe the coupling between climate and economic growth require fast modules for the different parts of the Earth system, which includes the GIS (e.g. Hulme et al., 1995). A fast ice sheet model also would be useful for exploring the effects of uncertain model parameters on hindcasts and projections of the ice sheet's behavior (Robinson et al., 2011; Applegate et al., 2012). Simplified models have proven their usefulness in modeling other aspects of the climate system, notably the El Niño-Southern Oscillation (Cane and Zebiak, 1985) and the meridional overturning circulation (Stommel, 1961; Keller et al., 2007).

To help address these needs, we present the GLISTEN (GreenLand Ice SheeT ENhanced) model. This model is based on GRANTISM, a one-dimensional ice sheet model model by Pattyn (2006). GLISTEN resolves many processes that are important for the real ice sheet. We update the original GRANTISM model with improved treatments of surface ablation and basal temperatures, and we include a parameterization of the Zwally effect (Zwally et al., 2002; Parizek and Alley, 2004). These treatments are highly parameterized, which allows for very quick model evaluation.

In this paper, we first provide a brief overview of the processes that affect GIS behavior and then provide a complete description of the GLISTEN model. We indicate specifically where GLISTEN is simplified relative to more complex three-dimensional ice sheet models and where GLISTEN differs from GRANTISM. We then show that GLISTEN successfully imitates a three-dimensional, shallow-ice model (SICOPOLIS; http://sicopolis.greveweb.net; Greve, 1997; Greve et al., 2011) and can reproduce paleo- and instrumental observations. Finally, we discuss how this model can be extended and implemented in IAMs.

## 2 A brief overview of ice sheet models

The GLISTEN model presented in this paper represents many processes considered important for the GIS. An illustration of some of these processes is shown in Fig. 1, with glacier motion occuring as a result of internal deformation and basal sliding across the bedrock. Accumulation of ice and snow also primarily occurs at the center of the ice sheet, while ablation mainly occurs at the outer edges. This model is still considerably simplified, but it provides a rapid means of exploring GIS behavior that can be compared with more complex ice sheet models.

Perhaps the most complex components of an ice sheet model are the routines that calculate ice flow. The deformation of glacial ice is often assumed to follow a power-law for fluid flow with an exponent of ~3 (Glen, 1955; Nye, 1957; Cuffey and Kavanaugh, 2011, and references therein; cf. Goldsby and Kohlstedt, 2001); however, ice sheet ice is softer than the pure ice used in laboratory experiments, so a prefactor is used to match predictions from Glen's flow law to observed behavior (e.g. Rutt et al., 2009). Many current ice sheet models solve the equations of ice flow using the shallow-ice approximation (Hutter, 1983) and finite-difference solution methods over a grid that has a constant spacing in the horizontal plane but is scaled to ice thickness in the vertical direction. Examples of these shallow-ice models include SICOPOLIS (Greve, 1997; Greve et al., 2011) and Glimmer-CISM (Rutt et al., 2009). Both simpler and more complex solution methods exist. Velocities can be integrated vertically (e.g. Calov and Marsiat, 1998), leading to a simpler problem. A few models use finite elements instead of finite differences, allowing refinement of the model mesh in crucial areas (e.g. Larour et al., 2012; Leng et al., 2012). Higher-order models resolve stress components that are neglected by the shallow-ice approximation (Kirchner et al., 2011), but usually have significantly higher computing costs (e.g. Price et al., 2011; cf. Pollard and DeConto, 2009). Examples of these higher-order models include ISSM (Larour et al., 2012), Elmer/Ice (Seddik et al., 2012), and some versions of Glimmer-CISM (Price et al., 2011). One promising approach involves applying full-Stokes solution methods only where they are necessary to maintain accuracy (Seroussi et al., 2010).

The dynamics of ice flow are fundamentally different in ice streams and ice shelves than in places where the ice moves more slowly (MacAyeal et al., 1989; Kirchner et al., 2011). In slowly-moving grounded ice, deformation is controlled by vertical stresses; in ice streams and ice shelves, longitudinal stresses dominate. Ice margins in contact with water are highly vulnerable to mass loss from calving or basal melting. Removal of ice shelves also can cause tributary glaciers to speed up (e.g. Schmeltz et al., 2002; Scambos et al., 2004; Dupont and Alley, 2005). Shallow-ice models simply neglect the problem of enhanced flow; others use the "shallow shelf approximation" in regions of fast flow (e.g. Bueler and Brown, 2009). Hybrid, higher-order, and full-Stokes models treat these features of the ice sheet "automatically," rather than requiring a separate module for fast-flow regions. Calving and ice shelf basal processes represent areas of active research (e.g. Alley et al., 2008; Walker et al., 2009).

Ice flow is sensitive to local temperature (Paterson and Budd, 1982; Greve and Blatter, 2009), and some thermal energy enters ice sheets from the bed (e.g. Dahl-Jensen and Gundestrup, 1987; Greve, 2005). Warmer ice deforms more readily than cold ice, and water-ice mixtures (sometimes known as “temperate ice”) are softer still. Most models treat the advection and diffusion of thermal energy, but only a very few allow formation of water-ice mixtures (e.g. SICOPOLIS; Greve, 1997). Energy is transported between spatially fixed points in an ice sheet model both by diffusion and by advection; for example, a large amount of cold precipitation falling on the upper reaches of an ice sheet will pass through the ice body as a cold wave.

Where grounded ice is not frozen to its bed, it can slide. The effectiveness of this process depends on the areal concentration and size of asperities (e.g. Weertman, 1957), as well as basal water pressure and sediment availability. Many models adopt a Weertman-type sliding law (Weertman, 1957; Hindmarsh and le Meur, 2001; Greve, 2005) that accounts for basal temperature and the relative importance of shear and overburden stresses. Sediment production and transport is typically neglected (for an exception, see Pollard and DeConto, 2003). Identifying the best form of the basal sliding law is the subject of active discussion (for a review, see e.g. Alley, 2000).

The great weight of ice sheets presses the crustal surface downward, and removal of this load by ice melting allows the crustal surface to rebound (Peltier, 2004; Greve and Blatter, 2009). This process is usually modeled as an adjustment towards a new equilibrium with some relaxation timescale. Some models use the local lithosphere relaxation approach (LLRA), which considers only the history of ice thickness in individual grid cells; the more complex elastic lithosphere relaxation approach (ELRA) accounts for ice masses in adjacent cells (Greve and Blatter, 2009).

The surface mass balance of ice sheets is treated simply in many models, but this group of processes is likely more important than ice flow over geological time scales. Precipitation falls everywhere on ice sheets, but more ice melts than falls as snow near sea level and at lower latitudes. Both sublimation and melting remove ice from ice sheets, but sublimation requires much more energy per unit ice mass (Rupper and Roe, 2008). Most models handle precipitation by pattern scaling of gridded, modern-day precipitation data or reanalysis output (e.g. Stone et al., 2010). The modeled local temperature (e.g. Fausto et al., 2009) determines how much of this precipitation falls as rain or snow (Marsiat, 1994; Bales, 2009). Ablation is usually taken to be a linear function of the integrated surface temperature above freezing (the positive degree-day method; Reeh, 1991; Braithwaite, 1995; Calov and Greve, 2005), likely neglecting sublimation. Many models allow refreezing of melted precipitation within the snowpack, often following Reeh (1991). Despite the simplicity of the surface mass balance specifications used by many models, the surface mass balance exerts a strong control on the ice margin position; given the thinness of ice near the margin, ice flow is relatively minor in comparison to mass balance (Letreguilly et al., 1991; Greve, 1997; Alley et al., 2010).

Recent work suggests that ice sheet surface mass balance influences ice velocities through the "Zwally effect" (Zwally et al., 2002; Bartholomew et al., 2010). On the Greenland ice sheet, meltwater collects in ponds. This meltwater exploits existing weaknesses in the ice to drill downwards, sometimes reaching the bed (Alley et al., 2008, 2010). The meltwater transports thermal energy from the ice sheet surface to greater depths, and may lubricate the bed, allowing faster sliding. The importance of this mechanism is still open to question; Parizek and Alley (2004) found in a modeling experiment that its effect was relatively small unless a larger part of the bed became available for meltwater lubrication (see also Greve and Otsu, 2007).

Most ice sheet models are driven by user-specified curves for temperature and background sea level, derived from geological data or from climate model runs (e.g. Greve et al., 2011). Precipitation is tied to temperature through an exponential relationship based on the Clausius-Clapeyron equation and ice core data (Huybrechts and de Wolde, 1999; cf. Cuffey and Clow, 1997; van der Veen, 2002). A few studies have





TCD
6, 2751–2788, 2012

incorporated regional climate models into ice sheet models (e.g. Robinson et al., 2010, 2011).

## 3 Model description

The GLISTEN model is a one-dimensional flow-line dynamic ice sheet model written in Fortran 90 and is based upon the GRANTISM model of Pattyn (2006). This simplified model is based on mass and momentum conservation laws and invokes the shallow-ice approximation so that vertical shearing at the bed of a large ice mass is balanced by the driving stress within. In this section we provide a description of the GLISTEN model and note the differences with the precursor GRANTISM model accordingly.

### 3.1 Model equations and numerical solution methods

For an ice sheet with thickness $H$, we can express the conservation of mass with the continuity equation

$$\frac{\partial H}{\partial t} = -\nabla\left(\bar{u}H\right) + \dot{a}, \tag{1}$$

where $\bar{u}$ is the vertical mean horizontal velocity, $\dot{a}$ is the surface mass balance between ice accumulation and ablation, and $t$ is time. (We consider mass balance at the surface only and neglect melting at the base of the ice sheet.) We separate the horizontal velocity into two components $\bar{u} = \bar{u}_\mathrm{d} + u(b)$, where $\bar{u}_\mathrm{d}$ is the flow that results from internal deformation and $u(b)$ is basal sliding at the height $b$ of the bedrock topography. We assume a form of $\bar{u}_\mathrm{d}$ derived by Paterson (1994) as

$$\bar{u}_\mathrm{d} = \frac{2\eth}{n+2} A(T) H \tau_\mathrm{d}^n, \tag{2}$$

where $n$ is the flow law exponent, $\tau_\mathrm{d}$ is the driving stress in the ice sheet, $A(T)$ is a temperature-dependent flow parameter (defined by Eq. 19), and $\eth$ is a deformation





TCD
6, 2751–2788, 2012

A computationally efficient model for the Greenland ice sheet

J. Haqq-Misra et al.

Title Page
Abstract | Introduction
Conclusions | References
Tables | Figures
◂◂ | ▸▸
◂ | ▸
Back | Close
Full Screen / Esc
Printer-friendly Version
Interactive Discussion

parameter fixed at $\mathfrak{d} = 1$. We likewise define the basal velocity $u(b)$ in terms of the driving stress follwing Greve et al. (2011) so that

$$u(b) = \mathfrak{b} S_\mathrm{b} e^{T_\mathrm{b}/\gamma} \frac{\tau_\mathrm{d}^p}{(\rho_\mathrm{i} g H)^q}, \tag{3}$$

where $p$ and $q$ are sliding exponents, $\gamma$ is a sub-melt sliding parameter, $T_\mathrm{b}$ is basal temperature (defined by Eq. 28), $\rho_\mathrm{i}$ is a constant ice density, $g$ is gravitational acceleration, and $\mathfrak{b}$ is a basal sliding parameter fixed at $\mathfrak{b} = 1$.

We represent the "Zwally effect" with a sliding coefficient $S_\mathrm{b}$ that depends on mass balance $\dot{a}$ (defined by Eqs. 20 and 27) according to

$$S_\mathrm{b} = \begin{cases} Z_f S_0 & \text{for } \dot{a} < 0 \\ S_0 & \text{for } \dot{a} \geq 0 \end{cases}, \tag{4}$$

where $S_0$ is a sliding coefficient constant and the Zwally effect parameter $Z_f$ is fixed at $Z_f = 1.1$.

We invoke the shallow-ice approximation because our model is applicable for large ice masses, which allows us to write the driving stress as

$$\tau_\mathrm{d} = -\rho_\mathrm{i} g H \nabla h, \tag{5}$$

where $h = H + b$ is surface elevation of the ice sheet. This set of Eqs. (1), (2), (3), and (5) forms the basis of our ice sheet model.

We construct a numerical solution to our set of model equations by first expressing the continuity equation as a diffusive equation by substituting $\bar{u}H = -D\nabla h$ in Eq. (1) so that

$$\frac{\partial H}{\partial t} = \nabla(D\nabla h) + \dot{a}. \tag{6}$$





TCD
6, 2751–2788, 2012

We can combine Eqs. (2), (3), (5), and (6) to solve for the diffusivity $D$:

$$D = H^{n+2}|\nabla h|^{n-1}(\rho_\mathrm{i} g)^n \left(\frac{2\mathfrak{d}}{n+2}A(T)\right) + H^{p-q+1}|\nabla h|^{p-1}(\rho_\mathrm{i} g)^{p-q}\left(\mathfrak{b} S_\mathrm{b} e^{T_\mathrm{b}/\gamma}\right). \tag{7}$$

This diffusive continuity equation (6) is then described using a semi-implicit numerical scheme to express the ice thickness $H_t$ and $H_{t+1}$ at time steps $t$ and $t+1$ as

$$H_{t+1} = H_t + \nabla\left[D_t\left(\varpi\nabla\left(H_{t+1}+b_{t+1}\right)+(1-\varpi)\nabla h_t\right)\right]\Delta t + \dot{a}\Delta t, \tag{8}$$

where $\varpi$ denotes a weighting between implicit and explicit terms.[1] (Note that we have also assumed $h_t = H_t + b_t$ in Eq. 8.) In this case, the diffusivity (Eq. 7) has been rewritten as $D_t$ to include a time step:

$$D_t = H_t^{n+2}|\nabla h_t|^{n-1}(\rho_\mathrm{i} g)^n \left(\frac{2\mathfrak{d}}{n+2}A(T)\right) + H_t^{p-q+1}|\nabla h_t|^{p-1}(\rho_\mathrm{i} g)^{p-q}\left(\mathfrak{b} S_\mathrm{b} e^{T_\mathrm{b}/\gamma}\right). \tag{9}$$

If we specify $N$ grid points along a flow-line so that the set of $i$ grid points are numbered as $i = 1, 2, \ldots, N-1, N$, then we can express Eq. (8) in terms of a tridiagonal system of equations

$$\alpha_{i,t} H_{i-1,t+1} + \beta_{i,t} H_{i,t+1} + \gamma_{i,j} H_{i+1,t+1} = \delta_{i,t}, \tag{10}$$

which can be solved using the tridiagonal matrix algorithm, also known as the Thomas algorithm (Press et al., 2007). We first discretize our length scale as $\Delta x$ so that the scaling of Eq. (8) can be expressed as

$$\nabla\left(D_t \nabla h\right)\Delta t \sim \frac{\Delta t}{(2\Delta x)^2} \equiv \Delta_{tx}, \tag{11}$$

[1] A value of $\varpi = 0$ corresponds to an explicit scheme, $\varpi = 1$ to a semi-implicit scheme, and $\varpi = \frac{1}{2}$ to a Crank-Nicholson scheme.





TCD
6, 2751–2788, 2012

where we have defined the symbol $\Delta_{tx}$ to represent our discrete element.[2] The complete numerical formulation of our system of equations in the form of Eq. (10) is then

$$\alpha_{i,t} = -\omega\Delta_{tx}\left(D_{i,t} + D_{i-1,t}\right), \tag{12}$$

$$\beta_{i,t} = 1 + \omega\Delta_{tx}\left(D_{i-1,t} + 2D_{i,t} + D_{i+1,t}\right), \tag{13}$$

$$\gamma_{i,t} = -\omega\Delta_{tx}\left(D_{i,t} + D_{i+1,t}\right), \text{ and} \tag{14}$$

$$\delta_{i,t} = -\Delta_{tx}\left(D_{i,t} + D_{i-1,t}\right)\left[\omega\left(b_{i,t+1} - b_{i-1,t+1}\right) + (1-\omega)\left(h_{i,t} - h_{i-1,t}\right)\right] \tag{15}$$

$$+ \Delta_{tx}\left(D_{i,t} + D_{i+1,t}\right)\left[\omega\left(b_{i+1,t+1} - b_{i,t+1}\right) + (1-\omega)\left(h_{i+1,t} - h_{i,t}\right)\right] \tag{16}$$

$$+ H_{i,t} + \dot{a}\Delta t. \tag{17}$$

We use a semi-implicit scheme of $\omega = 1$, a flow law exponent of $n = 3$, and sliding law exponents of $p = 3$ and $q = 2$. A list of these non-dimensional parameters and other scaling factors used in the GLISTEN model is given in Table 1, while physical constants and global dimensional parameters are given in Table 2.

## 3.2 Model parameterizations

In the GLISTEN model, ice flow is thermomechanically coupled to ambient temperature, even though temperature is not explicitly calculated within the ice sheet. The background forcing temperature $T_\mathrm{f}$ (with units of °C) describes the anomalous temperature relative to present conditions, and the background sea level forcing $H_\mathrm{sl}$ describes the anomalous sea level rise relative to today. GLISTEN (as well as GRANTISM) defines ice temperature $T$ (with units of K) in terms of the background forcing temperature through an empirical relationship:

$$T = \begin{cases} T_\mathrm{f} + 263.15 & \text{for } T_\mathrm{f} < 0 \\ 0.5T_\mathrm{f} + 263.15 & \text{for } T_\mathrm{f} \geq 0 \end{cases}. \tag{18}$$

[2] Note that this term appears in Eqs. (19), (20), and (22) of Pattyn (2006) as $\Delta t / \left(2(\Delta x)^2\right)$.

This allows us to define the flow parameter $A(T)$ with the empirical expression

$$A(T) = m\left(\frac{1}{B_0}\right)^n \exp\left[\frac{3C}{(T_r - T)^K} - \frac{Q}{RT}\right], \tag{19}$$

where $B_0$ is a flow constant, $R$ is the universal gas constant, $Q$ is the activation energy for creep, $T_r$ is a reference temperature, and $m$, $C$, and $K$ are flow parameters.

The surface mass balance $\dot{a}$ between surface accumulation $\dot{a}_{acc}$ and surface ablation $\dot{a}_{abl}$ over the ice sheet is defined as $\dot{a} = \dot{a}_{acc} + \dot{a}_{abl}$. Surface accumulation in all grid cells is taken to be the average from regional climate model output (Ettema et al., 2009) along our model flow-line. All precipitation is assumed to fall as snow. This mean value for surface accumulation is constant along the flow-line and represented by $\bar{a}_0$. Surface accumulation then can be written as

$$\dot{a}_{acc} = \bar{a}_0 \times \mathfrak{s}^{T_f^\star}, \tag{20}$$

where $\mathfrak{s}$ is fixed at $\mathfrak{s} = 1.0533$, $T_f^\star = T_f$ for $T_f \leq 0$, and $T_f^\star = 0$ otherwise.

Mean annual surface temperatures $T_{ma}$ and July mean surface temperatures $T_{ms}$ are parameterized as functions of altitude $h$, latitude $\phi$, and longitude $\lambda$ according to Fausto et al. (2009) so that

$$T_{ma} = 41.83 - 6.309h - 0.7189\phi + 0.0672\lambda + T_f, \text{ and} \tag{21}$$

$$T_{ms} = 14.70 - 5.426h - 0.1585\phi + 0.0518\lambda + T_f, \tag{22}$$

where we specify the latitude $\phi = 72^\circ$. If we further assume that annual temperature $T_{ac}$ varies sinusoidally with time $t$ so that

$$T_{ac}(t) = T_{ma} + (T_{ms} - T_{ma})\cos\frac{2\pi t}{A}, \tag{23}$$

where $A = 1\,\text{yr}$, then we can calculate the number of positive degree days using the semi-analytic solution developed by Calov and Greve (2005). We first define the





TCD

6, 2751–2788, 2012

A computationally efficient model for the Greenland ice sheet

J. Haqq-Misra et al.

complementary error function as

$$\mathrm{erfc}(x) = \frac{2}{\sqrt{\pi}} \int_x^{\infty} \exp\left(-\tilde{x}^2\right) \mathrm{d}\tilde{x} \tag{24}$$

so that the number of positive degree days in one year can be written as

$$\mathrm{PDD} = \int_0^A \left[ \frac{\sigma}{\sqrt{2\pi}} \exp\left(-\frac{T_{\mathrm{ac}}^2}{2\sigma^2}\right) + \frac{T_{\mathrm{ac}}}{2} \mathrm{erfc}\left(-\frac{T_{\mathrm{ac}}}{\sigma\sqrt{2}}\right) \right] \mathrm{d}t, \tag{25}$$

(Calov and Greve, 2005) where $\sigma$ is standard deviation of the annual cyclic temperature from the mean annual temperature. We express $\sigma$ analytically by applying the definition of standard deviation to Eqs. (21–23) and integrating by parts to result in

$$\sigma = \sqrt{\frac{1}{A} \int_0^A (T_{\mathrm{ac}} - T_{\mathrm{ma}})^2 \, \mathrm{d}t} = \frac{T_{\mathrm{ms}} - T_{\mathrm{ma}}}{\sqrt{2}}, \tag{26}$$

which accounts for time variation in temperature by noting that $\partial T_{\mathrm{ms}}/\partial t = \partial T_{\mathrm{ma}}/\partial t = \mathrm{d}T_{\mathrm{f}}/\mathrm{d}t$ (i.e. both $T_{\mathrm{ms}}$ and $T_{\mathrm{ma}}$ change at the same rate). This parameterization allows us to write surface ablation in terms of PDD and a positive degree day factor $\mathfrak{p}$ as

$$\dot{a}_{\mathrm{abl}} = \mathfrak{p}\mathrm{PDD}, \tag{27}$$

where the factor $\mathfrak{p}$ is fixed at $\mathfrak{p} = -2 \times 10^{-3}\,\mathrm{m\,day^{-1}}$. This simple balance between mass accumulation and loss represents processes such as surface snowfall, surface melting, percolation of meltwater within the ice sheet, and refreezing.

Although our simple model cannot explicitly resolve temperature profiles across the entire ice sheet, we can calculate a value for the basal temperature $T_{\mathrm{b}}$ by using Fick's





TCD

6, 2751–2788, 2012



Title Page
Abstract Introduction
Conclusions References
Tables Figures
◂ ▸
Back Close
Full Screen / Esc
Printer-friendly Version
Interactive Discussion

Second Law

$$\frac{\partial T_b}{\partial t} = \kappa \frac{\partial^2 T_b}{\partial \phi^2} \tag{28}$$

to represent thermal diffusion in terms of the diffusion coefficient $\kappa$. For ice, we can write

$$\kappa = \frac{k_i}{\rho_i C_i}, \tag{29}$$

where $k_i$ is the thermal conductivity of ice and $C_i$ is the thermal capacity of ice. We assume that the temperature at the top of the ice sheet is equal to the mean annual temperature $T_{ma}$ in Eq. (21), which allows us to solve for basal temperature $T_b(t,\phi)$ as a function of time and location along the flow-line:

$$T_b = T_{ma} \operatorname{erfc}\left(\frac{H}{2\sqrt{\kappa t}}\right) + \mathfrak{q}, \tag{30}$$

where the term $\mathfrak{q}$ represents a geothermal energy flux and initially is fixed at $\mathfrak{q} = 0\,\mathrm{K}$.

Bedrock deflection follows a relaxation scheme with a time scale $\theta$ to determine local isostatic equilibrium:

$$\frac{\partial b}{\partial t} = \frac{1}{\theta}\left(b_0 - b - \frac{\rho_i}{\rho_m} H\right), \tag{31}$$

where $\rho_m$ is the mantle density. Here $b_0$ is the isostatically adjusted bedrock elevation that would result by removing the current load of ice defined as

$$b_0 = b_{obs} + \frac{\rho_i}{\rho_m} H_{obs}, \tag{32}$$

where $b_{obs}$ and $H_{obs}$ are the bedrock height and ice height used as initial conditions, respectively. The starting distributions of bedrock topography $b_{obs}$ and ice thickness





TCD
6, 2751–2788, 2012

$H_{obs}$ in these simulations follow a $\Delta x = 36$ km resampled grid spacing based on observations (Letreguilly et al., 1991). We also prevent the ice sheet from expanding into the ocean by specifying an ice thickness $H = 0$ at the Eastern and Western boundaries where $b < H_{sl}$ so that the bedrock is beneath sea level.

## 4 Pre-calibration

The physical parameterizations described above depend on several uncertain parameters that can generate substantial variation in model behavior. We perform a pre-calibration of GLISTEN by adjusting the eight variable parameters listed in Table 3 in order to obtain a model that is capable of reproducing geological data and modern observations (Letreguilly et al., 1991; Rignot et al., 2008; Alley et al., 2010). We first use GLISTEN to emulate the behavior of a three-dimensional ice sheet model. We then use this solution as the initial state for a series of seven experiments for pre-calibration according to three possible constraints on GIS behavior (listed in Table 4).

We calculate a score for each model calculation by defining a loss function based on changes in the volume of the GIS $\Delta V$ (in meters of sea level equivalent) with respect to the present. In general, this loss function is expressed in terms of the mean value $\mu_i$ and standard deviation $\sigma_i$ of the $i$th pre-calibration constraint as a sum over all $N$ constraints:

$$\mathcal{L} = \sum_{i=0}^{N} \left\{ -\log \left[ \frac{1}{\sigma_i \sqrt{2\pi}} \exp \left( - \left( \frac{\Delta V_i - \mu_i}{\sigma_i \sqrt{2}} \right)^2 \right) \right] \right\}. \tag{33}$$

The score in Eq. (33) is expressed as a negative logarithm of probability so that model calculations can be compared with one another through minimization and combined as a sum.

We use the differential evolution algorithm (Storn and Price, 1997; Price et al., 2005) to generate a population of model calculations and select an optimal set of parameters.





TCD
6, 2751–2788, 2012

Differential evolution (DE) is an iterative genetic algorithm for optimization that takes a parent population of model parameter configurations, forms a mutant population of new configurations, and selects among these candidates for fitness (by minimizing the loss function Eq. 33) to form a new child population. This process is repeated until the DE algorithm reaches a statistically steady state to yield an optimized set of parameters.

We begin by pre-calibrating GLISTEN so as to emulate the behavior of the SICOPOLIS three-dimensional ice sheet model. We use the forcing data and volume calculations from run #29 of Applegate et al. (2012), which yields the best match to the estimated volume of the modern GIS (Bamber et al., 2001). As constraints, we compare the ice volume of GLISTEN to the SICOPOLIS calculation at three locations along the time series: (1) an average over a warm period in the Eemian (from 118 500 to 115 000 yr ago; the actual timing of the Eemian peak warmth is probably somewhat older, around 125–127 ka, but we use this range here because it is the warmest quasi-Eemian period in the GRIP ice core record); (2) an average during the Last Glacial Maximum (from 20 000 to 19 000 yr ago); and (3) the last time step at present day. All three of these constraints assume a standard deviation of one meter of sea level equivalent volume. We initialize GLISTEN with a present-day GIS profile and force the model using the same temperature forcing $T_f$, sea level forcing $H_{sl}$ as the SICOPOLIS calculation. The result of this pre-calibration of GLISTEN to SICOPOLIS is shown in Fig. 2, which also shows that the GLISTEN emulation is a significantly better fit to SICOPOLIS than GRANTISM. Although the emulation is not able to precisely replicate the behavior of SICOPOLIS, it follows the major trends and provides a place to begin further pre-calibration experiments.

We next define a series of seven pre-calibration experiments that are defined according to the combinations of three sets of constraints from data. The first constraint is based on expert assessment of GIS volume changes at different times in the past (Alley et al., 2011) and provides a range for sea level rise from Greenland ice during the Eemian, the Last Glacial Maximum, and present day. These paleo-constraints are shown as grey boxes in Fig. 3, where the width of the box is the time period considered and the height of the box is the range of sea level rise (see Alley et al., 2010). The second constraint is based on instrumental data (Rignot et al., 2008) from recent decades of the mass balance of the GIS. These five constraints are shown as grey bars in Fig. 4, where the height of the bar is one standard deviation for mass balance. The third constraint is based on the similarity of the calculated ice sheet profile to the observed GIS profile; we use the parameter estimation method described by Olson et al. (2012) as the loss function for this constraint. The constraint on the GIS profile is shown as the solid black line in Fig. 5, which is the present-day geography interpolated to a $\Delta x = 36$ km grid. The combinations of these three constraints yield the seven experiments that are outlined in Table 4.

We initialize the model with a present-day GIS profile and use a temperature forcing $T_f$ and sea level forcing $H_{sl}$ from GRIP, the Greenland Ice Core Project (Dansgaard et al., 1993; Johnsen et al., 1997; shown in the top two panels of Fig. 2), with a timestep $\Delta t = 100$ yr. The best fits to the data sets considered in experiments EXP1 through EXP7 are shown in Fig. 3 as sea level rise due to changes in the GIS over the past 125 000 yr. The seven model configurations show varied behavior with time, although they all stay within range of the three paleo-constraints on sea level rise. It is interesting to note that even the experiments that do not consider the paleo-constraints (EXP4, EXP5, and EXP6) still behave similarly to the other configurations. The seven GLISTEN experiments, however, provide geologically consistent trajectories for GIS volume that show a more dynamic response than the original GRANTISM implementation.

We then continue integrating the GLISTEN model using temperature forcing $T_f$ from instrumental records over the past 150 yr (Vinther et al., 2006), a constant sea level $H_{sl} = 0$, and a timestep $\Delta t = 1$ yr. The optimal parameter configurations for EXP1 through EXP7 are shown in Fig. 4 as the GIS mass balance over the past 150 yr. All these experiments show a close agreement to one another and fall within one standard deviation of the instrumental data constraints. Three of these pre-calibration experiments (EXP3, EXP5, and EXP7) did not consider the constraints from instrumental data, yet even these calculations show agreement with recent records. GLISTEN appears to accurately represent the recent instrumental record using a variety of parameter configurations.

Upon completing this pre-calibration, the final GIS profile for the seven experiments is shown in Fig. 5. All seven profiles are similar to one another, including the three experiments (EXP2, EXP6, and EXP7) that did not consider the constraint on the final GIS profile. The optimal parameter configurations for EXP1 through EXP7 are given in Table 3, which includes the prior ranges of each parameter and the SICOPOLIS emulation. All of these model configurations show a range in parameter values, although almost none of them approach the lower or upper prior ranges. These experiments (EXP1 through EXP7, plus the SICOPOLIS emulation) describe eight potential ways to configure the parameters in GLISTEN.

## 5 Discussion

The pre-calibration experiments described above provide several potential ways to configure the GLISTEN model. These model configurations compare with results from the three-dimensional ice sheet model SICOPOLIS and satisfy constraints based on assessed paleo-ice volume changes and instrumental records. For these reasons, GLISTEN may be useful as a tool to model the behavior of the GIS during time periods from the Eemian to the present.

GLISTEN's advantage over three-dimensional models is that it features much shorter computation time. We illustrate this in Fig. 6, which shows the CPU time required to compute a 125 000 yr paleo-calculation, for which GLISTEN takes about half a second and SICOPOLIS takes a few days. The computational speed of GLISTEN makes it an ideal tool for use in IAMs. Simulations with IAMs often use large numbers of ensemble members ($>10^5$) in order to consider a wide range of possibilities for climate change and therefore require a reasonable timescale (<6 months) for computation (e.g. McInerney and Keller, 2008; Goes et al., 2011; McInerney et al., 2011), shown as the green shaded area in Fig. 6. For such ensemble sizes, GLISTEN would require weeks to months of CPU time, whereas SICOPOLIS would require decades or more to perform the same calculations. In this case, one-dimensional flow-line models are a more practical tool than more complex models. The behavior of the GIS is relevant for IAMs because changes in the volume of the GIS contribute to changes in sea level. Although three-dimensional ice sheet models would be far too time consuming, GLISTEN provides a rapid way to simulate GIS behavior for use in IAMs and other applications.

In summary, the full GLISTEN model is able to reproduce historical trends in the GIS from ice core and instrumental data. This model is simplified relative to three-dimensional models, such as SICOPOLIS, but it provides the advantage of rapid computational speed.

## 6 Conclusions

The GLISTEN one-dimensional flow-line model provides a computationally efficient tool for calculating changes in the GIS over the past 125 000 yr and can be configured using several sets of observational constraints and, consequently, several parameter configurations. The GLISTEN model can compute changes in the GIS at several orders of magnitude faster than three-dimensional ice sheet models. This makes GLISTEN an ideal candidate for implementation into IAMs to incorporate the dependence of GIS changes on sea level. In future work we will perform a full calibration of GLISTEN and incorporate it as a module in an IAM.

## Appendix A

### Changes from GRANTISM

GLISTEN is a direct descendent of GRANTISM by Pattyn (2006), and most of the basic equations and numerical methods are identical between the two models. Nearly





TCD
6, 2751–2788, 2012

all parameters are identical between GLISTEN and GRANTISM, as well (with the one exception that GRANTISM uses a value of $\rho_i = 910\,\mathrm{kg\,m^{-3}}$ for the density of ice). We have, however, made several changes to physical parameterizations in the model that differ from those used in GRANTISM. In particular, the representation of mass balance in GLISTEN is analytically defined in terms of the number of positive degree days at a particular location along the GIS flow-line, which is a substantial improvement upon the simplified parameterization used in GRANTISM. GLISTEN also implements an improved representation of basal sliding, which includes the "Zwally effect", and basal temperature. Below we describe the specific components of GRANTISM that differ from those in GLISTEN.

The expression for basal sliding in GRANTISM differs from that in the GLISTEN implementation (c.f. Eq. 3) and can be written as

$$u(b) = A_b \frac{\tau_d^p}{Z^\star}, \tag{A1}$$

where $A_b$ is related to the flow parameter as

$$A_b = \frac{1}{2} A(T) \times 10^6. \tag{A2}$$

Here $Z^\star$ is the height of the ice above surface buoyancy $Z^\star$, which is defined as

$$Z^\star = H + \frac{\rho_s}{\rho_i} \min\left[(b - H_{sl}), 0\right], \tag{A3}$$

where $\rho_s$ is the density of seawater. The eustatic sea level $H_{sl}$ is also prescribed in GRANTISM as a function of $T_f$ and with maximum lower bound so that

$$H_{sl} = \max\{\min[15T_f, 0], -150\}. \tag{A4}$$





TCD
6, 2751–2788, 2012

The representation of mass balance in GRANTISM also differs from the mass balance scheme used by GLISTEN. Surface accumulation in GRANTISM follows a second-order polynomial fit by Pattyn (2006) to the data of Ohmura and Reeh (1991) as

$$\dot{a}_{\mathrm{acc}} = \left(-2.46257 + 0.1367\lambda - 0.0016\lambda^2\right) \times 1.0533^{T_f^\star}, \qquad \text{(A5)}$$

with units of $\mathrm{m\,yr^{-1}}$ ice equivalent (c.f. Eq. 20). Additionally, the form of the mean summer surface temperature (Eq. 22) differs in GRANTISM and is parameterized as

$$T_{\mathrm{ms}} = -7.2936 - 0.006277h + T_{\mathrm{f}}. \qquad \text{(A6)}$$

(Note that Eq. 15 of Pattyn, 2006, takes a slightly truncated form with $T_{\mathrm{ms}} = -7.29 - 0.006277h + T_{\mathrm{f}}$, although the full equation above appears in the code for GRANTISM.) Surface ablation in GRANTISM likewise takes a simpler form than Eq. (27) because it is only dependent on $T_{\mathrm{ms}}$ and not on an annual cycle. The expression for surface ablation in GRANTISM follows

$$\dot{a}_{\mathrm{abl}} = \begin{cases} \max\left[-1.4T_{\mathrm{ms}}, -10\right] & \text{for } T_{\mathrm{ms}} \geq 0 \\ 0 & \text{for } T_{\mathrm{ms}} < 0 \end{cases}, \qquad \text{(A7)}$$

where a minimum ablation limit of $-10\,\mathrm{m\,yr^{-1}}$ is imposed (c.f. Eq. 27).

GRANTISM predicts significantly larger growth of the GIS over the past 125 000 yr in Fig. 3 when compared to any of our pre-calibration experiments or to SICOPOLIS. This suggests that GRANTISM may be limited in its ability to simulate dynamic responses to the GIS over geologic timescales. GRANTISM is more accurate at representing recent perturbations in the GIS, as shown by the similarity between GRANTISM and the seven pre-calibration curves in Fig. 4. This suggests to us that GRANTISM may be a useful tool for modeling recent changes in temperature.

*Acknowledgements.* We thank Roman Olson for his assistance with parameter estimation for the ice sheet profile. This research was supported in part by the US Department of Energy, Office of Science, Biological and Environmental Research Program, Integrated Assessment Program, through Grant No. DE-SC0005171, as well as the Penn State Center for Climate Risk Management. All errors and opinions are our own.

## References

Alley, R. B.: Continuity comes first: recent progress in understanding subglacial deformation, in: Deformation of Glacial Materials, edited by: Maltman, A. J., Hubbard, B., and Hambrey, M. J., Geol. Soc. Spec. Publ., 176, 171–179, 2000.

Alley, R. B., Horgan, H. J., Joughin, I., Cuffey, K. M., Dupont, T. K., Parizek, B. R., Anandakrishnan, S., and Bassis, J.: A simple law for ice-shelf calving, Science, 322, 1344, doi:10.1126/science.1162543, 2008.

Alley, R. B., Andrews, J. T., Brigham-Grette, J., Clarke, G. K. C., Cuffey, K. M., Fitzpatrick, J. J., Funder, S., Marshall, S. J., Miller, G. H., Mitrovica, J. X., Muhs, D. R., Otto-Bliesner, B. L., Polyak, L., and White, J. W. C.: History of the Greenland ice sheet: paleoclimate insights, Quaternary Sci. Rev., 29, 1728–1756, 2010.

Applegate, P. J., Kirchner, N., Stone, E. J., Keller, K., and Greve, R.: An assessment of key model parametric uncertainties in projections of Greenland Ice Sheet behavior, The Cryosphere, 6, 589–606, doi:10.5194/tc-6-589-2012, 2012.

Bales, R. C., Guo, Q., Shen, D., McConnell, J. R., Guoming, D., Burkhart, J. F., Spikes, V. B., Hanna, E., and Cappelen, J.: Annual accumulation for Greenland updated using ice core data developed during 2000–2006 and analysis of daily coastal meteorological data, J. Geophys. Res., 114, D06116, doi:10.1029/2008JD011208, 2009.

Bamber, J. L., Layberry, R. L., and Gogineni, S. P.: A new ice thickness and bed data set for the Greenland ice sheet, 1. Measurement, data reduction, and errors, J. Geophys. Res., 106, 33773–33780, 2001.

Bartholomew, I., Nienow, P., Mair, D., Hubbard, A., King, M. A., and Sole, A.: Seasonal evolution of subglacial drainage and acceleration in a Greenland outlet glacier, Nat. Geosci., 3, 408–411, 2010.





TCD
6, 2751–2788, 2012

Braithwaite, R. J.: Positive degree-day factors for ablation on the Greenland ice sheet studied by energy-balance modelling, J. Glaciol., 41, 153–160, 1995.
Bueler, E. and Brown, J.: Shallow shelf approximation as a “sliding law” in a thermomechanically coupled ice sheet model, J. Geophys. Res., 114, F03008, doi:10.1029/2008JF001179, 2009.
Calov, R. and Greve, R.: A semi-analytical solution for the positive degree-day model with stochastic temperature variations, J. Glaciol., 51, 173–175, 2005.
Calov, R. and Marsiat, I.: Simulations of the Northern Hemisphere through the last glacial-interglacial cycle with a vertically integrated and a 3-D thermomechanical ice sheet model coupled to a climate model, Ann. Glaciol., 27, 169–176, 1998.
Cane, M. A. and Zebiak, S. E.: A theory for El Niño and the southern oscillation, Science, 228, 1085–1087, 1985.
Cuffey, K. M. and Clow, G. D.: Temperature, accumulation, and ice sheet elevation in Central Greenland through the last deglacial transition, J. Geophys. Res., 102, 26383–26396, 1997.
Cuffey, K. M. and Kavanaugh, J. L.: How nonlinear is the creep deformation of polar ice? A new field assessment, Geology, 39, 1027–1030, 2011.
Dahl-Jensen, D. and Gundestrup, N. S.: Constitutive properties of ice at Dye-3, Greenland, in: The Physical Basis of Ice Sheet Modelling, edfited by: Waddington, E. and Walder, J., IAHS-AISH P., 170, 31–43, 1987.
Dansgaard, W., Johnsen, S., Clausen, H., Dahl-Jensen, D., Gundestrup, N., Hammer, C., Hvidberg, C., Steffensen, J., Sveinbjornsdottir, A., and Jouzel, J.: Evidence for general instability of past climate from a 250-kyr ice-core record, Nature, 364, 218–220, 1993.
Dupont, T. K. and Alley, R. B.: Assessment of the importance of ice-shelf buttressing to ice-sheet flow, Geophys. Res. Lett., 32, L0450, doi:10.1029/2004GL022024, 2005.
Ekholm, S.: A full coverage, high-resolution, topographic model of Greenland computed from a variety of digital elevation data, J. Geophys. Res., 101, 21961–21972, 1996.
Fausto, R. S., Ahlstrom, A. P., van As, D., Boggild, C. E., and Johnsen, S. J.: A new present-day temperature parameterization for Greenland, J. Glaciol., 55, 95–105, 2009.
Glen, J. W.: The creep of polycrystalline ice, P. R. Soc. Lond. A, 228, 519–538, doi:10.1098/rspa.1955.0066, 1955.
Goes, M., Keller, K., and Tuana, N.: The economics (or lack thereof) of aerosol geoengineering, Climatic Change, 109, 719–744, 2011.
Goldsby, D. L. and Kohlstedt, D. L.: Superplastic deformation of ice: experimental observations, J. Geophys. Res., 106, 11017–11030, 2001.





TCD
6, 2751–2788, 2012

A computationally efficient model for the Greenland ice sheet

J. Haqq-Misra et al.

Greve, R.: Application of a polythermal three-dimensional ice sheet model to the Greenland ice sheet: response to steady-state and transient climate scenarios, J. Climate, 10, 901–918, 1997.
Greve, R.: On the response of the Greenland ice sheet to greenhouse climate change, Climatic Change, 46, 289–303, 2000.
Greve, R.: Relation of basal measured temperatures and the spatial distribution of the geothermal heat flux for the Greenland Ice Sheet, Ann. Glaciol., 42, 424–432, 2005.
Greve, R. and Blatter, H.: Dynamics of Ice Sheets and Glaciers, Monograph Series Advances in Geophysical and Environmental Mechanics and Mathematics, 2009.
Greve, R. and Otsu, S.: The effect of the north-east ice stream on the Greenland ice sheet in changing climates, The Cryosphere Discuss., 1, 41–76, doi:10.5194/tcd-1-41-2007, 2007.
Greve, R., Saito, F., and Abe-Ouchi, A.: Initial results of the SeaRISE numerical experiments with the models SICOPOLIS and IcIES for the Greenland ice sheet, Ann. Glaciol., 52, 23–30, 2011.
Hindmarsh, R. C. A. and Le Meur, E.: Dynamical processes involved in the retreat of marine ice sheets, J. Glaciol., 47, 271–279, 2001.
Hulme, M., Raper, S. C. B., and Wigley, T. M. L.: An integrated framework to address climate change (ESCAPE) and further developments of the global and regional climate modules (MAGICC), Energ. Policy, 23, 347–355, 1995.
Hutter, K.: Theoretical Glaciology: Material Science of Ice and the Mechanics of Glaciers and Ice Sheets, D. Reidel, Dordrecht, 1983.
Huybrechts, P. and de Wolde, J.: The dynamic response of the Greenland and Antarctic ice sheets to multiple-century climatic warming, J. Climate, 12, 2169–2188, 1999.
Johnsen, S., Clausen, H., Dansgaard, W., Gundestrup, N., Hammer, C., Andersen, U., Andersen, K., Hvidberg, C., Dahl-Jensen, D., and Steffensen, J.: The $\delta$18O record along the Greenland Ice Core Project deep ice core and the problem of possible Eemian climatic instability, J. Geophys. Res., 102, 26397–26410, 1997.
Keller, K., Deutsch, C., Hall, M. G., and Bradford, D. F.: Early detection of changes in the North Atlantic meridional overturning circulation: implications for the design of ocean observation systems, J. Climate, 20, 145–157, 2007.
Kirchner, N., Hutter, K., Jakobsson, M., and Gyllencreutz, R.: Capabilities and limitations of numerical ice sheet models: a discussion for Earth-scientists and modelers, Quaternary Sci. Rev., 30, 3691–3704, 2011.





TCD
6, 2751–2788, 2012

A computationally efficient model for the Greenland ice sheet

J. Haqq-Misra et al.

Larour, E., Seroussi, H., Morlighem, M., and Rignot, E.: Continental scale, high order, high spatial resolution ice sheet modeling using the Ice Sheet System Model (ISSM), J. Geophys. Res., 17, F01022, doi:10.1029/2011JF002140, 2012.

Leng, W., Ju, L., Gunzburger, M., Price, S., and Ringler, T.: A parallel high-order accurate finite element nonlinear Stokes ice sheet model and benchmark experiments, J. Geophys. Res., 117, F01001, doi:10.1029/2011JF001962, 2012.

Letreguilly, A., Huybrechts, P., and Reeh, N.: Steady-state characteristics of the Greenland ice sheet under different climates, J. Glaciol., 37, 149–157, 1991.

Lhomme, N., Clarke, G. K. C., and Marshall, S. J.: Tracer transport in the Greenland ice sheet: constraints on ice cores and glacial history, Quaternary Sci. Rev., 24, 173–194, 2005.

Lunt, D. J., de Noblet-Ducoudre, N., and Charbit, S.: Effects of a melted Greenland ice sheet on climate, vegetation, and the cryosphere, Clim. Dynam., 23, 679–694, 2004.

Lythe, M. B., Vaughan, D. G., and the Bedmap Consortium: Bedmap: a new ice thickness and subglacial topography model of Antarctica, J. Geophys. Res., 106, 11335–11351, 2001.

MacAyeal, D. M.: Large-scale ice flow over a viscous basal sediment: theory and application to Ice Stream B, Antarctica, J. Geophys. Res., 94, 4071–4087, 1989.

Marsiat, I.: Simulation of the Northern Hemisphere continental ice sheets over the last glacial-interglacial cycle: experiments with a latitude-longitude vertically integrated ice sheet model coupled to a zonally averaged climate model, Palaeoclimates, 1, 59–98, 1994.

McInerney, D. and Keller, K.: Economically optimal risk reduction strategies in the face of uncertain climate thresholds, Climatic Change, 91, 29–41, 2008.

McInerney, D., Lempert, R., and Keller, K.: What are robust strategies in the face of uncertain climate threshold responses?, Climatic Change, 112, 547–568, doi:10.1007/s10584-011-0377-1, 2011

Meehl, G. A., Stocker, T. F., Collins, W. D., Friedlingstein, A. T., Gaye, A. T., Gregory, J. M., Kitoh, A., Knutti, R., Murphy, J. M., and Noda, A.: Global climate projections, in: Climate Change 2007: The Physical Science Basis. Contribution of Working Group I to the Fourth Assessment Report of the Intergovernmental Panel on Climate Change, edited by: Solomon, S., Qin, D., Manning, M., Chen, Z., Marquis, M., Averyt, K. B., Tignor, M., and Miller, H. L., Cambridge University Press, 2007.

Mote, T. L.: Greenland surface melt trends 1973–2007: evidence of a large increase in 2007, Geophys. Res. Lett., 34, L22507, doi:10.1029/2007GL031976, 2007.



Discussion Paper | Discussion Paper | Discussion Paper | Discussion Paper |

Nye, J. F.: The distribution of stress and velocity in glaciers and ice-sheets, P. R. Soc. Lond. A, 239, 113–133, doi:10.1098/rspa.1957.0026, 1957.
Olson, R., Sriver, R., Goes, M., Urban, N. M., Matthews, H. D., Haran, M., and Keller, K.: A climate sensitivity estimate using Bayesian fusion of instrumental observations and an Earth System model, J. Geophys. Res., 117, D04103, doi:10.1029/2011JD016620, 2012.
Parizek, B. R. and Alley, R. B.: Implications of increased Greenland surface melt under global-warming scenarios: ice sheet simulations, Quaternary Sci. Rev., 23, 1013–1027, 2004.
Paterson, W. S. B. and Budd, W. F.: Flow parameters for ice sheet modeling, Cold Reg. Sci. Technol., 6, 175–177, 1982.
Pattyn, F.: GRANTISM: an Excel(TM) model for Greenland and Antarctic ice-sheet response to climate changes, Comput. Geosci., 32, 316–325, 2006.
Peltier, W. R.: Global glacial isostasy and the surface of the ice-age Earth: the ICE-5G (VM2) model and GRACE, Annu. Rev. Earth Pl. Sc., 32, 111–149, 2004.
Pollard, D. and DeConto, R. M.: Antarctic ice and sediment flux in the Oligocene simulated by a climate-ice sheet-sediment model, Palaeogeogr. Palaeocl., 198, 53–67, 2003.
Pollard, D. and DeConto, R.: Modelling West Antarctic ice sheet growth and collapse through the past five million years, Nature, 458, 329–333, 2009.
Press, W. H., Teukolsky, S. A., Vetterling, W. T., and Flannery, B. P.: Numerical Recipes: The Art of Scientific Computing, 3rd edn., Cambridge University Press, 2007.
Price, K. V., Storn, R. M., and Lampinen, J. A.: Differential evolution: a practical approach to global optimization, Springer-Verlag, New York, 2005.
Price, S. F., Payne, A. J., Howat, I. M., and Smith, B. E.: Committed sea-level rise for the next century from Greenland ice sheet dynamics during the past decade, P. Natl. Acad. Sci. USA, 108, 8978–8983, 2011.
Reeh, N.: Parameterization of melt rate and surface temperature on the Greenland ice sheet, Polarforschung, 59, 113–128, 1898.
Rignot, E., Box, J., Burgess, E., and Hanna, E.: Mass balance of the Greenland ice sheet from 1958 to 2007, Geophys. Res. Lett., 35, L20502, doi:10.1029/2008GL035417, 2008.
Robinson, A., Calov, R., and Ganopolski, A.: An efficient regional energy-moisture balance model for simulation of the Greenland Ice Sheet response to climate change, The Cryosphere, 4, 129–144, doi:10.5194/tc-4-129-2010, 2010.

Robinson, A., Calov, R., and Ganopolski, A.: Greenland ice sheet model parameters constrained using simulations of the Eemian Interglacial, Clim. Past, 7, 381–396, doi:10.5194/cp-7-381-2011, 2011.
Rupper, S. and Roe, G.: Glacier changes and regional climate: a mass and energy balance approach, J. Climate, 21, 5384–5401, 2008.
Rutt, I. C., Hagdorn, M., Hulton, N. R. J., and Payne, A. J.: The Glimmer community ice-sheet model, J. Geophys. Res.-Earth, 114, F02004, doi:10.1029/2008JF001015, 2009.
Scambos, T. A., Bohlander, J. A., Shuman, C. A., and Skvarca, P.: Glacier acceleration and thinning after ice shelf collapse in the Larsen B embayment, Antarctica, Geophys. Res. Lett., 31, L18402, doi:10.1029/2004GL020670, 2004.
Schmeltz, M., Rignot, E., Dupont, T. K., and MacAyeal, D. R.: Sensitivity of Pine Island Glacier, West Antarctica, to changes in ice-shelf and basal conditions: a model study, J. Glaciol., 48, 552–558, 2002.
Seddik, H., Greve, R., Zwinger, T., Gillet-Chaulet, F., and Gagliardini, O.: Simulations of the Greenland ice sheet 100 yr into the future with the full Stokes model Elmer/Ice, J. Glaciol., 58, 209, 427–440, 2012.
Seroussi, H. L., Rignot, E. J., Morlighem, M., Larour, E. Y., ben Dhia, H., and Aubry, D.: A numerically optimized, computationally efficient method to couple full-Stokes and simpler models of ice sheet flow, in: American Geophysical Union Fall Meeting, Abstract C32A-07, 2010.
Stommel, H.: Thermohaline convection with two stable regimes of flow, Tellus, 13, 224–230, 1961.
Stone, E. J., Lunt, D. J., Rutt, I. C., and Hanna, E.: Investigating the sensitivity of numerical model simulations of the modern state of the Greenland ice-sheet and its future response to climate change, The Cryosphere, 4, 397–417, doi:10.5194/tc-4-397-2010, 2010.
Storn, R. and Price, K.: Differentia evolution: a simple and efficient heuristic for global optimization over continuous spaces, J. Global Optim., 11, 341–359, 1997.
Tarasov, L. and Peltier, W. R.: Greenland glacial history, borehole constraints, and Eemian extent, J. Geophys. Res., 108, 2143, doi:10.1029/2001JB001731, 2003.
Toniazzo, T., Gregory, J. M., and Huybrechts, P.: Climatic impact of a Greenland deglaciation and its possible irreversibility, J. Climate, 17, 21–33, 2004.
Torinesi, O., Fily, M., and Genthon, C.: Variability and trends of the summer melt period of Antarctic ice margins since 1980 from microwave sensors, J. Climate, 16, 1047–1060, 2003.





TCD
6, 2751–2788, 2012

A computationally efficient model for the Greenland ice sheet

J. Haqq-Misra et al.

van der Veen, C. J.: Polar ice sheets and global sea level: how well can we predict the future?, Global Planet. Change, 32, 165–194, 2002.
Velicogna, I.: Increasing rates of ice mass loss from the Greenland and Antarctic ice sheets revealed by GRACE, Geophys. Res. Lett., 36, LI19503, doi:10.1029/2009GL040222, 2009.
Vinther, B., Andersen, K., Jones, P., Briffa, K., and Cappelen, J.: Extending Greenland temperature records into the late eighteenth century, J. Geophys. Res., 111, D11105, doi:10.1029/2005JD006810, 2006.
Walker, R. T., Dupont, T. K., Holland, D. M., Parizek, B. R., and Alley, R. B.: Initial effects of oceanic warming on a coupled ocean-ice shelf-ice stream system, Earth Planet. Sci. Lett., 287, 483–487, 2009.
Weertman, J.: On the sliding of glaciers, J. Glaciol., 3, 33–38, 1957.
Zwally, H. J., Abdalati, W., Herring, T., Larson, K., Saba, J., and Steffen, K.: Surface melt-induced acceleration of Greenland Ice-Sheet flow, Science, 297, 218–222, 2002.





TCD
6, 2751–2788, 2012

A computationally efficient model for the Greenland ice sheet

J. Haqq-Misra et al.

**Table 1.** List of non-dimensional parameters and scaling factors.

| Parameter | Value | Definition | First Appears in Eq. |
|---|---|---|---|
| $n$ | 3 | Flow law exponent | (2) |
| $p$ | 3 | Sliding law exponent | (3) |
| $q$ | 2 | Sliding law exponent | (3) |
| $\varpi$ | 1 | Semi-implicit weighting | (8) |
| $m$ | 7.5 | Flow parameter | (19) |
| $C$ | 0.16612 | Flow parameter | (19) |
| $K$ | 1.17 | Flow parameter | (19) |
| $\mathfrak{d}$ | 1 | Variable deformation parameter | (2) |
| $\mathfrak{b}$ | 1 | Variable basal sliding parameter | (3) |
| $\mathfrak{s}$ | 1.0533 | Variable surface accumulation parameter | (20) |
| $Z_f$ | 1.1 | Zwally effect parameter | (4) |





TCD
6, 2751–2788, 2012

**Table 2.** List of constants and global parameters.

| Parameter | Value | Units | Definition | First Appears in Eq. |
|---|---|---|---|---|
| $g$ | 9.81 | $\mathrm{m\,s^{-2}}$ | Gravitational acceleration | (3) |
| $S_0$ | 11.2 | $\mathrm{m\,yr^{-1}\,Pa^{-1}}$ | Sliding coefficient constant | (4) |
| $\gamma$ | 1 | $^{\circ}\mathrm{C}$ | Sub-melt sliding parameter | (3) |
| $\theta$ | 3000 | yr | Asthenosphere relaxation time | (31) |
| $\rho_\mathrm{i}$ | 917 | $\mathrm{kg\,m^{-3}}$ | Ice density | (3) |
| $\rho_\mathrm{m}$ | 3300 | $\mathrm{kg\,m^{-3}}$ | Mantle density | (31) |
| $\rho_\mathrm{s}$ | 1028 | $\mathrm{kg\,m^{-3}}$ | Seawater density | (A3) |
| $k_\mathrm{i}$ | 2.2 | $\mathrm{W\,m^{-1}\,K^{-1}}$ | Thermal conductivity of ice | (29) |
| $C_\mathrm{i}$ | 2000 | $\mathrm{J\,kg^{-1}\,K^{-1}}$ | Thermal capacity of ice | (29) |
| $R$ | 8.31 | $\mathrm{J\,mol^{-1}\,K^{-1}}$ | Universal gas constant | (19) |
| $Q$ | $7.88 \times 10^4$ | $\mathrm{J\,mol^{-1}}$ | Activation energy for creep | (19) |
| $B_0$ | 2.207 | $\mathrm{Pa\,yr^{1/n}}$ | Flow constant | (19) |
| $T_\mathrm{r}$ | 273.39 | K | Reference temperature | (19) |
| $\bar{a}_0$ | 0.41 | $\mathrm{m\,yr^{-1}}$ | Average surface accumulation | (20) |
| $\Delta x$ | 5 | km | Discrete length step | (11) |
| $\Delta t$ | 1, 10, 20, 100 | yr | Discrete time step | (8) |
| $\mathfrak{p}$ | $-2 \times 10^{-3}$ | $\mathrm{m\,day^{-1}}$ | Variable positive degree day parameter | (27) |
| $\mathfrak{q}$ | 0 | K | Variable basal temperature parameter | (30) |





TCD
6, 2751–2788, 2012

**Table 3.** Estimated parameters and their prior ranges for the pre-calibration experiments.

| Parameter | $\mathfrak{d}$ | $\mathfrak{b}$ | $\mathfrak{s}$ | $\mathfrak{q}$ | $\mathfrak{p}$ | $\bar{a}_0$ | $\theta$ | $Z_f$ |
|---|---|---|---|---|---|---|---|---|
| First Appears in Eq. | (2) | (3) | (20) | (30) | (27) | (20) | (31) | (4) |
| Lower Bound | 0.1 | 0.1 | 0.99 | −10.0 | $-2.5 \times 10^{-3}$ | 0.205 | 1500 | 0.55 |
| Upper Bound | 10.0 | 10.0 | 1.2640 | 10.0 | $-1.0 \times 10^{-2}$ | 0.82 | 6000 | 2.2 |
| SICOPOLIS Emulation | 6.9947 | 5.6669 | 1.1693 | −7.5545 | $-2.9 \times 10^{-3}$ | 0.6161 | 5126 | 1.9624 |
| EXP1 | 1.5355 | 1.0718 | 1.0841 | 2.0214 | $-2.6 \times 10^{-3}$ | 0.4119 | 3928 | 0.8849 |
| EXP2 | 1.0443 | 8.3725 | 1.1516 | 0.4480 | $-3.0 \times 10^{-3}$ | 0.4372 | 2322 | 0.5224 |
| EXP3 | 2.0934 | 8.9303 | 1.0765 | 0.5036 | $-2.9 \times 10^{-3}$ | 0.4435 | 5082 | 0.4953 |
| EXP4 | 1.3195 | 4.1531 | 1.0761 | 1.1807 | $-2.6 \times 10^{-3}$ | 0.3738 | 2329 | 0.5330 |
| EXP5 | 0.8948 | 4.4749 | 1.0616 | 1.0128 | $-3.3 \times 10^{-3}$ | 0.3794 | 1585 | 0.5501 |
| EXP6 | 1.0291 | 3.6380 | 1.1429 | 1.1609 | $-2.7 \times 10^{-3}$ | 0.4041 | 5630 | 0.2503 |
| EXP7 | 1.9064 | 1.4645 | 1.1277 | 2.2770 | $-2.7 \times 10^{-3}$ | 0.4223 | 5085 | 0.6351 |





TCD

6, 2751–2788, 2012

**Table 4.** Summary of the pre-calibration experiments.

| | EXP1 | EXP2 | EXP3 | EXP4 | EXP5 | EXP6 | EXP7 |
|---|---|---|---|---|---|---|---|
| Assessed paleo-ice volume changes (Alley et al., 2010) | T | T | T | F | F | F | T |
| Estimated yearly total mass balance (Rignot et al., 2008) | T | T | F | T | F | T | F |
| Observed ice thicknesses along model flow-line (Letreguilly et al., 1991) | T | F | T | T | T | F | F |





TCD
6, 2751–2788, 2012

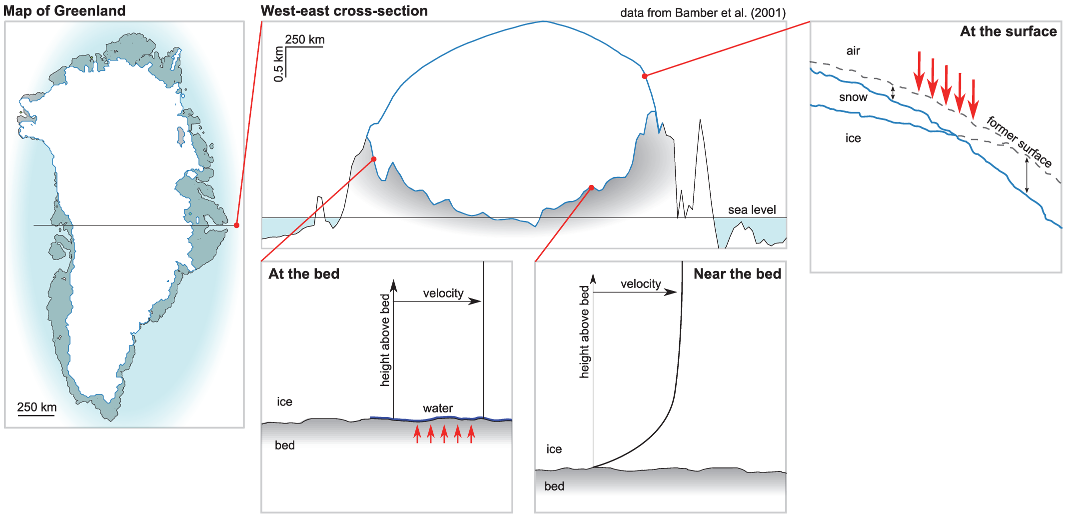


**Fig. 1.** Cartoon of selected processes important to ice sheet behavior. Ice sheet models represent the falling of snow onto the high, cold parts of the ice sheet and the translation of this snow as ice to the margins where it melts. Transport is accomplished through sliding where the bed is thawed ("at the bed," lower left) and through internal deformation of the ice ("near the bed," lower right). At the surface, melting causes the surface of the ice sheet to lower. The figure does not show calving where the ice margin enters the water or the "Zwally effect" (Zwally et al., 2002).

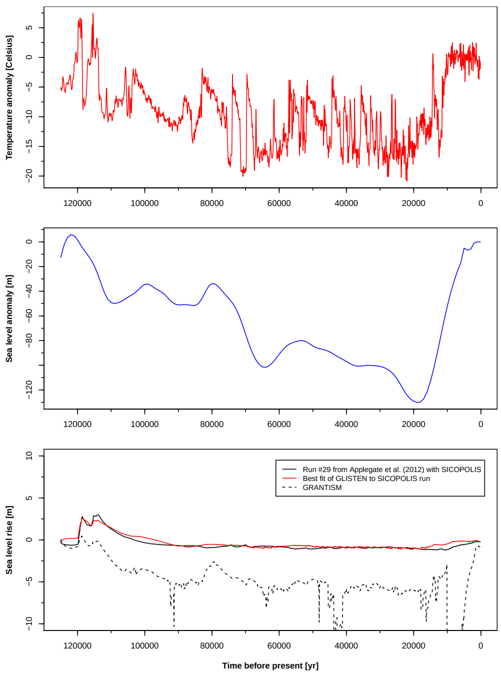


**Fig. 2.** Forcings used to model ice sheet evolution over the last 125 000 yr, and demonstration that GLISTEN is able to match results from a three-dimensional ice sheet model (SICOPOLIS; Greve, 1997; Greve et al., 2011). The top panel shows Greenland annual mean temperature anomaly reconstructed from oxygen isotopes in the GRIP ice core (Dansgaard et al., 1993; Johnsen et al., 1997). The middle panel shows sea level anomaly reconstructed from ocean sediment core oxygen isotopes (Imbrie et al., 1984). The bottom panel shows the best fit of GLISTEN model (red line) to results from run #29 from Applegate et al. (2012) using SICOPOLIS (black line). The SICOPOLIS run was generated using the forcing data in the top two panels. For reference, we show results from the original GRANTISM model (dashed line; Pattyn, 2006), which also uses the forcing data shown in the top two panels.

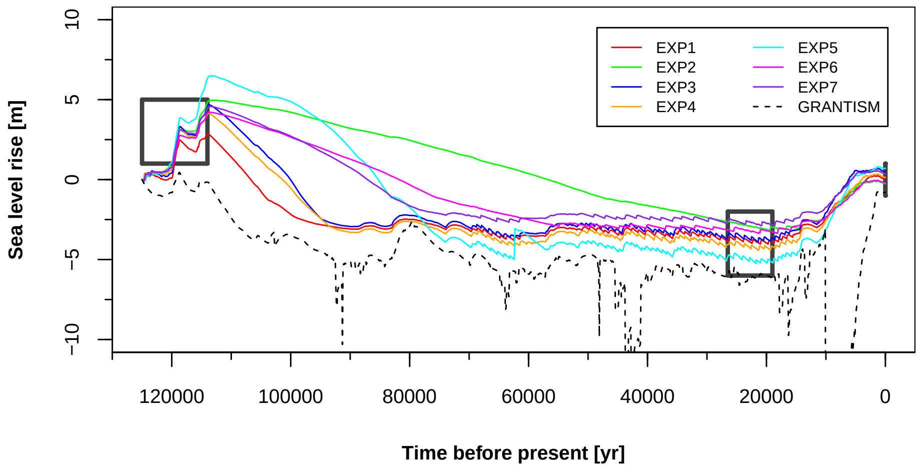


**Fig. 3.** Sea level rise from the Greenland Ice Sheet over the past 125 000 yr, where the colored curves show pre-calibration calculations EXP1 through EXP7 (see Table 4), and the dashed black curve shows calculations with the original GRANTISM configuration. Assessed changes in ice volume (Alley et al., 2010, their Fig. 13), relative to the present day, are shown in grey with horizontal lines indicating the time period for averaging and vertical lines showing the range of sea level rise.

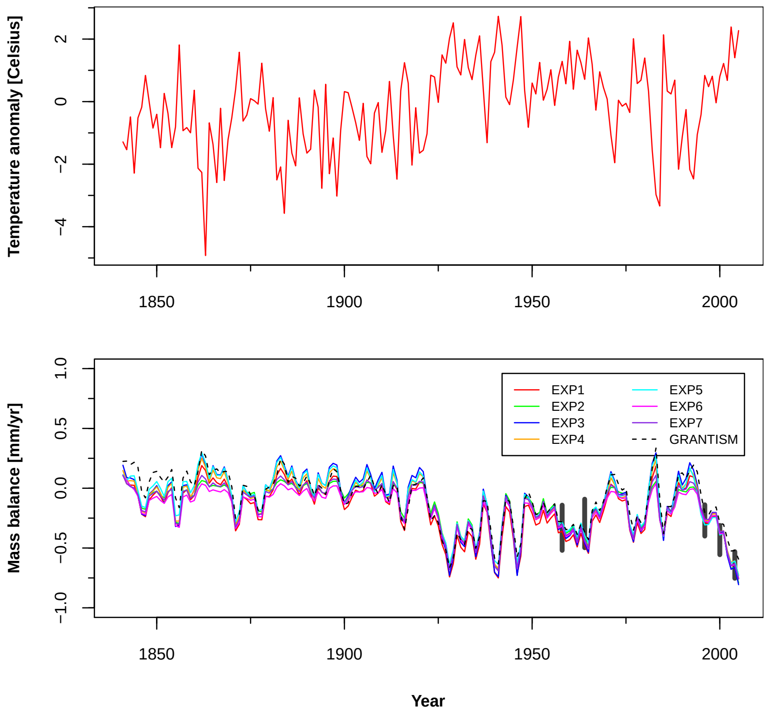


**Fig. 4.** Temperature forcing used to model ice sheet evolution over the past 150 yr and mass balance for the Greenland Ice Sheet calculated with GLISTEN. The top panel shows the Greenland annual mean temperature anomaly from instrumental records (Vinther et al., 2006). In the bottom panel, the colored curves show pre-calibration calculations EXP1 through EXP7 (see Table 4), and the dashed black curve shows calculations with the original GRANTISM configuration. Five constraints from instrumental data (Rignot et al., 2008) are shown in grey with vertical lines drawn at one standard deviation.

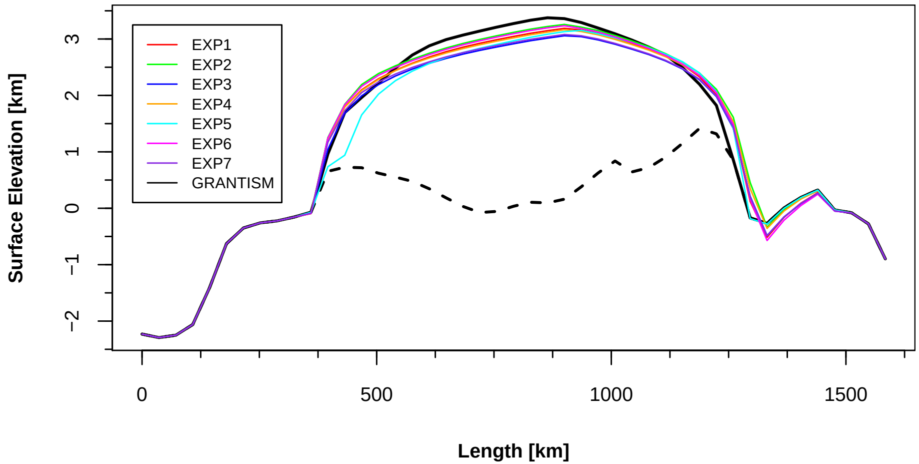


**Fig. 5.** Final GIS profile from pre-calibration calculations EXP1 through EXP7 (see Table 4). The solid black curve shows the GIS profile for GRANTISM, and the dashed black curve shows the elevation of bedrock (interpolated from Letreguilly et al., 1991).





TCD
6, 2751–2788, 2012

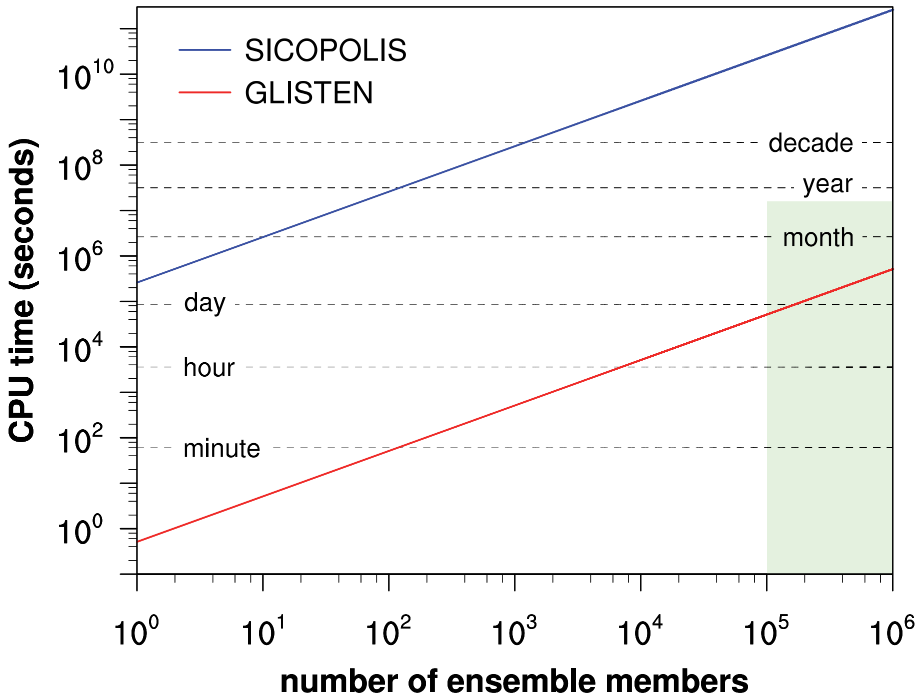


**Fig. 6.** CPU time for 125 000 yr ice sheet calculations using the one-dimensional GLISTEN model (red line) and the three-dimensional SICOPOLIS model (blue line) as a function of the desired number of model runs. The green rectangle represents the requirements imposed by many integrated assessment models to run a large number (>$10^5$) of model runs in a reasonable time-scale (<6 months). GLISTEN is able to complete simulations with a large number of ensemble members in a time frame of weeks to months, whereas SICOPOLIS would take several decades or longer of computational time to complete the same task.





TCD
6, 2751–2788, 2012